Autonomous biogeochemical floats detect significant carbon dioxide outgassing in the high-latitude Southern Ocean

Alison R. Gray[1], Kenneth S. Johnson[2], Seth M. Bushinsky[3], Stephen C. Riser[1], Joellen L. Russell[4], Lynne D. Talley[5], Rik Wanninkhof[6], Nancy L. Williams[7], and Jorge L. Sarmiento[3]

Alison R. Gray, argray@uw.edu

[1]School of Oceanography, University of Washington, Seattle, Washington 98195, USA.

[2]Monterey Bay Aquarium Research Institute, Moss Landing, California 95039, USA.

[3]Program in Atmospheric and Oceanic Sciences, Princeton University, Princeton, New Jersey 08544, USA.

This article has been accepted for publication and undergone full peer review but has not been through the copyediting, typesetting, pagination and proofreading process, which may lead to differences between this version and the Version of Record. Please cite this article as doi: 10.1029/2018GL078013

Although the Southern Ocean is thought to account for a significant portion of the contemporary oceanic uptake of carbon dioxide (CO_2), flux estimates in this region are based on sparse observations that are strongly biased towards summer. Here we present new estimates of Southern Ocean air-sea CO_2 fluxes calculated with measurements from biogeochemical profiling floats deployed by the Southern Ocean Carbon and Climate Observations and Modeling (SOCCOM) project during 2014-2017. Compared to ship-based CO_2 flux estimates, the float-based fluxes find significantly stronger outgassing in the zone around Antarctica where carbon-rich deep waters upwell to the

[4]Department of Geosciences, University of Arizona, Tucson, Arizona 85721, USA.

[5]Scripps Institution of Oceanography, University of California San Diego, La Jolla, California 92093, USA.

[6]Atlantic Oceanographic and Meteorological Laboratory, National Oceanic and Atmospheric Administration, Miami, Florida 33149, USA.

[7]College of Earth, Ocean, and Atmospheric Sciences, Oregon State University, Corvallis, Oregon 97331 USA.

surface ocean. Although interannual variability contributes, this difference principally stems from the lack of autumn and winter ship-based observations in this high-latitude region. These results suggest that our current understanding of the distribution of oceanic CO_2 sources and sinks may need revision and underscore the need for sustained year-round biogeochemical observations in the Southern Ocean.

Keypoints:

- Measurements from biogeochemical profiling floats were used to estimate air-sea fluxes of carbon dioxide.
- Significant annual net outgassing of carbon dioxide was observed in the high-latitude Antarctic-Southern Zone.
- In this region, a large difference with previous estimates was found in winter when ship-based sampling is sparse.

1. Introduction

The Southern Ocean, the region south of 35°S surrounding Antarctica, has a remarkably strong influence on the Earth's climate in general and on the exchange of carbon between the ocean and atmosphere in particular [*Gruber et al.*, 2009]. Observation-based estimates of the contemporary air-sea flux of carbon dioxide (CO_2) typically find substantial net uptake in this region, with climatological values of -0.8 and -1.0 PgC y^{-1} estimated by *Takahashi et al.* [2009] and *Landschützer et al.* [2015], respectively (where negative denotes flux into the ocean). However, significant variability exists on interannual and decadal time scales [*Le Quéré et al.*, 2007; *Lenton et al.*, 2013; *Landschützer et al.*, 2015]. Most global climate models simulate a modern Southern Ocean CO_2 sink in the range of -0.5 to -1.3 PgC y^{-1} south of 35°S [*Nevison et al.*, 2016]. In addition, this region has accounted for nearly half of the global oceanic uptake of carbon emitted by anthropogenic activities over the past 125 years, according to an analysis of multiple coupled climate models [*Frölicher et al.*, 2015]. On longer time scales, changes to the Southern Ocean carbon flux have also been implicated in controlling glacial-interglacial cycles [*Sigman et al.*, 2010].

The importance of this region in the global carbon cycle stems from its unique circulation, in which the deep waters originating in both the Atlantic and the Indo-Pacific upwell to the surface ocean, largely adiabatically [*Lumpkin and Speer*, 2007; *Marshall and Speer*, 2012; *Talley*, 2013]. The upwelled waters are then transformed, either into intermediate waters that subduct and move northward in the upper ocean or into the densest bottom waters that are transported northward to fill the global abyssal ocean. Because they have been isolated from the atmosphere for hundreds of years, the upwelling

deep waters are naturally depleted in oxygen (O_2) and enriched in dissolved inorganic carbon (DIC) and macronutrients such as nitrate (NO_3), with negligible anthropogenic carbon concentrations. The transport of this water into the surface layer of the Southern Ocean therefore stimulates both a large release of natural carbon into the atmosphere and a significant uptake of anthropogenic carbon from the atmosphere [*Gruber et al.*, 2009]. The net uptake of total CO_2 (the sum of the natural and anthropogenic components) is thus determined by the balance between these two opposing fluxes.

Despite its impact on the climate system, the Southern Ocean remains one of the most poorly-sampled regions of the global ocean, especially with regard to biogeochemical variables such as nutrients, oxygen, and carbon. The observational datasets typically used to estimate air-sea CO_2 fluxes, consisting of underway ship-board measurements of the partial pressure of CO_2 in seawater (pCO_2^{ocn}), are sparse in both space and time in the Southern Ocean [*Bakker et al.*, 2016]. Outside of the Drake Passage [*Munro et al.*, 2015], relatively few data exist in the autumn and winter months when the extreme conditions of this area are largely prohibitive for ship-based sampling. In addition, modeling in this region is challenging due to the large variability at smaller scales and the complex interactions between the ocean, atmosphere, and cryosphere [*Meijers*, 2014].

With recent advances in sensor technologies, autonomous biogeochemical profiling floats are now capable of providing year-round measurements of O_2, NO_3, and pH in the upper 2000 m [*Johnson et al.*, 2017]. This study presents the first mean air-sea CO_2 fluxes estimated with observations from 35 of these floats deployed in the Southern Ocean during 2014-2017 as part of the SOCCOM project. After comparing the results to two widely-

used flux estimates computed from ship-based data, we examine potential causes of the significant disagreement found in the high-latitude portion of the Southern Ocean and discuss implications for our understanding of the Southern Ocean's role in the global carbon cycle.

2. Float-based Air-sea CO_2 Flux Estimates

Air-sea CO_2 fluxes were estimated using observations from 35 autonomous profiling biogeochemical floats operating from 1 May 2014 to 1 May 2017 in the Southern Ocean (Fig. 1; Table S1). In addition to collecting profiles of temperature (T) and salinity (S) in the upper 2000 m of the ocean every 5 or 10 days, these floats were equipped with state-of-the-art sensors to measure pH, NO_3, and dissolved O_2. All data were transmitted to shore in near real-time, along with a Global Positioning System (GPS) fix of the float location at the surface. Detailed information about the float data, including calibration processes, can be found in Text S1 [*Tengberg et al.*, 2006; *Johnson et al.*, 2013, 2015; *Wanninkhof et al.*, 2016; *Williams et al.*, 2016].

The pH data collected by the profiling floats (Fig. S1) were combined with total alkalinity (A_T) empirically estimated using the LIARv2 method [*Carter et al.*, 2018] (Fig. S2) to calculate $pCO_2{}^{ocn}$ in the surface layer (Fig. S3). All float data used in this study, including estimated A_T and calculated $pCO_2{}^{ocn}$ are publicly available [*Johnson et al.*, 2018]. Using these $pCO_2{}^{ocn}$ estimates, air-sea CO_2 flux F was computed along each float path (Fig. S4) according to

$$F = k\,K_0\,(\mathrm{pCO_2^{ocn}} - \mathrm{pCO_2^{atm}}). \tag{1}$$

The gas transfer velocity k was estimated using the parameterization of *Wanninkhof* [2014] and wind speed reanalysis data [ERA-Interim; *Kalnay et al.*, 1996]. The solubility K_0 of CO_2 was computed based on the measured T and S following *Weiss* [1974]. Measurements of atmospheric CO_2 from the Cape Grim Observatory were used to estimate the partial pressure of CO_2 in the atmosphere, pCO_2^{atm}. Different alkalinity estimates, wind speed products, atmospheric pressure estimates, and definitions of the ocean surface layer were used to gauge the sensitivity of F and the annual net fluxes computed below. In all cases, the resulting changes were much less than the associated uncertainty estimates. Further details about these tests and the methods used to compute pCO_2^{ocn} and CO_2 flux are given in Text S2 [*Perez and Fraga*, 1987; *Dickson*, 1990; *Lueker et al.*, 2000; *Lee et al.*, 2010; *de Boyer Montégut et al.*, 2004; *Dee et al.*, 2011; *Bentamya and Fillona*, 2012; *Zeebe and Wolf-Gladrow*, 2001; *Cavalieri et al.*, 1996]. In the remaining analysis, positive fluxes signify outgassing from the ocean to the atmosphere, and negative fluxes denote uptake by the ocean.

To estimate the total Southern Ocean carbon flux, the ocean south of 35°S was first divided into five regions corresponding to different oceanographic regimes (Fig. 1); methodological details given in Text S3 [*Orsi et al.*, 1995; *Roemmich and Gilson*, 2009]. The northernmost region, the Subtropical Zone (STZ), was characterized by warm, saline surface waters with nitrate concentrations less than 5 µmol kg^{-1}. Moving southward, the Subantarctic Zone (SAZ) was the region with deep winter mixed layers and surface waters that were cooler and fresher than those in the STZ. The Polar Frontal Zone (PFZ), which encompassed the northern part of the Antarctic Circumpolar Current, and the Antarctic-

Southern Zone (ASZ), which extended from the PFZ to the edge of the seasonally ice-covered zone, both had cold and fresh surface waters with large nitrate concentrations ($\geq$ 20 µmol kg^{-1} in the PFZ and $\geq$ 24 µmol kg^{-1} in the ASZ). In the southernmost seasonal ice zone (SIZ) the coldest surface waters and the largest seasonal salinity changes were observed. Floats in this region were capable of measuring under sea ice during winter [*Wong and Riser*, 2011].

Using these zones as the basis for sorting the float data, a mean seasonal cycle of air-sea CO_2 flux was constructed for each region. The fluxes calculated along each float path were averaged over every full month that the float collected data to give monthly mean fluxes. Each monthly mean estimate was then categorized into one of the five zones based on analysis of the float location relative to the mean regional boundaries, as well as the measured T, S, and NO_3 in the surface layer. Averaging all individual monthly mean flux estimates by zone and month produced mean seasonal cycles for the five zones (Fig. 2).

The overall pattern in the seasonality of CO_2 flux found here agrees with expectations of how temperature-driven changes in solubility compete with changes in DIC due to summertime biological uptake and wintertime resupply to the surface ocean [*Takahashi et al.*, 2002]. In the STZ, the float estimates showed strongest oceanic uptake of CO_2 in early winter and smaller fluxes into the ocean in late summer. Such a seasonal cycle is characteristic of a system controlled primarily by temperature-driven changes in CO_2 solubility. The seasonality of the SAZ is reversed, with uptake of CO_2 during the spring and summer, when NO_3 concentrations are lower (Fig. S5), followed by small outgassing fluxes of CO_2 and small increases in NO_3 concentrations in the winter. This pattern is consistent with

a regime that is more influenced by transport and biological processes than by seasonal temperature changes. The seasonal cycle in the PFZ is similar to the SAZ but shows more outgassing in the autumn and winter months, suggesting an increased influence of high-carbon upwelled waters. The mean seasonal cycle estimated from the ASZ floats was dominated by strong outgassing over most of the year, peaking in winter, followed by near-zero fluxes in December and January. That, together with NO_3 concentrations that are drawn down significantly in spring, suggests that the seasonal cycle in this zone is predominantly influenced by wintertime transport of DIC into the surface ocean and summertime biological uptake. In the SIZ, where ice cover suppresses wintertime air-sea CO_2 fluxes, the seasonal cycle showed significant oceanic uptake during the late spring through the summer, with a small net outgassing in the autumn before the formation of sea ice.

The annual net flux of carbon in each zone was estimated by integrating the mean seasonal cycle over one year and multiplying by the average area of each region, which assumes that these fluxes were representative of the entire region during the period 1 May 2014-1 May 2017 (Fig. 3; Table S2). The uncertainty estimates reported here, which represent ±1 standard error, account for both the variability observed within each region (which contributed ±0.01-0.02 PgC y^{-1} per zone) and the uncertainties associated with the flux calculation, including separate consideration of any possible biases in the float-based pCO_2^{ocn} estimates. Text S4 gives a detailed description of the uncertainty estimation methods [*Salstein et al.*, 2008; *Chaudhuri et al.*, 2013]. Both the STZ and the SAZ were found to be regions of oceanic uptake of carbon, with annual net fluxes of -0.35 ± 0.12 PgC

y^{-1} and -0.10 ± 0.14 PgC y^{-1}, respectively. The uptake in the STZ and SAZ was opposed by outgassing in the three zones south of the Subantarctic Front. Negligible annual net fluxes were estimated for the PFZ (0.01 ± 0.12 PgC y^{-1}) and SIZ (0.01 ± 0.06 PgC y^{-1}). In the ASZ, however, a substantial outgassing of 0.36 ± 0.11 PgC y^{-1} was estimated from the float observations.

3. Comparison to Ship-based Flux Estimates

The float-based fluxes were compared with two widely-used gridded CO_2 flux estimates based on shipboard pCO_2^{ocn} data: 1) a climatological estimate from *Takahashi et al.* [2009] (hereafter *Tak09*) and 2) a 35-year monthly estimate produced as part of the Global Carbon Budget 2017 [*Le Quéré et al.*, 2018] following the methodology of *Landschützer et al.* [2014] (hereafter *GCB17*). The results shown here for the *GCB17* estimate are an average over years 2007 to 2016, although the conclusions are unchanged if the average is instead computed over years 2014 to 2016. In both cases, monthly gridded fields were spatially interpolated to the float locations and the resulting subsampled datasets were used to compute mean seasonal cycles and annual net fluxes in the five zones (Fig. 2 and 3) following the same procedures as for the float data. The ship-based estimates were determined in this manner, before comparison to the float-based fluxes, to explicitly account for the incomplete spatial coverage of the floats. While further investigation is needed to quantify these impacts, the generally small difference between the subsampled ship-based flux and the total flux in any given region (Table S2) suggests the sampling of the floats does not introduce a substantial error in the resulting regional flux estimates. However, to minimize the influence of the spatio-temporal distribution of the float array

on the comparison to ship-based estimates, the remaining analysis considers only the subsampled ship-based fluxes.

In the STZ, the float-based flux agrees fairly well with the *Tak09* estimate both in the annual mean and over most of the seasonal cycle but gives less uptake in this region than the *GCB17* estimate (Figs. 2, 3; Table S2). Moving to the south, the SAZ flux computed from the floats shows less annual net uptake than is found in *Tak09* and *GCB17*, although the estimates mostly agree in late spring and summer. This pattern of better agreement in summer/ and spring than in autumn and winter holds in the PFZ, where the ship-based estimates find a net uptake but the float-based estimate shows a small net outgassing (that is not distinguishable from zero given the uncertainties). In the high-latitude ASZ, where the monthly mean float-based fluxes diverge substantially from the ship-based fluxes, the float estimates exhibit much stronger outgassing in the autumn and winter and much less uptake in the summer. These differences lead to significant disagreement in the annual net fluxes in this region, with the ship-based estimates giving near-zero fluxes and the float-based fluxes finding 0.36 ± 0.11 PgC y^{-1} released to the atmosphere. In the SIZ, the float-based annual net fluxes are not significantly different from the ship-based estimates, although the amplitude of the seasonal cycle was much reduced in the latter.

Although the 0.36 PgC y^{-1} difference in the ASZ stands out, the float-based estimates are higher than the ship-based fluxes in almost all regions. This widespread difference could arise if the float-based estimates of pCO_2^{ocn}, calculated from measured pH and estimated A_T, were biased high compared to directly-measured pCO_2^{ocn}. To examine this possibility, estimates of pCO_2^{ocn} from the floats were compared to all data from the

Surface Ocean CO_2 Atlas (SOCAT) v5 [*Bakker et al.*, 2016] within 25 km and 1 day of the float profile. To further ensure that the waters measured by the float were similar to those measured by the underway ship-based system, comparisons were retained only if the mean sea surface temperatures associated with the two estimates were within 0.3°C. The resulting comparison (Fig. 4) shows that the float-based pCO_2^{ocn} estimates agree reasonably well with the ship-based measurements given the associated uncertainties. On average, the float-based estimates were 3.6 ±3.4 µatm higher than the ship-based pCO_2^{ocn}.

This comparison, together with a thorough analysis of uncertainty in pCO_2^{ocn} calculated from float-measured pH and estimated A_T [*Williams et al.*, 2017], indicate that the float-derived pCO_2^{ocn} may be biased high by approximately 3.5 µatm. Such systematic errors (those which affect all float estimates in the same way and thus are not reduced by averaging data from multiple floats) could stem from uncertainties in seawater carbonate system thermodynamics [*Johnson et al.*, 2016; *Williams et al.*, 2017] or from biases in the float-measured O_2 used to adjust the pH data [*Johnson et al.*, 2017]. To account for this possibility, the flux results presented here were calculated with a Monte Carlo simulation that applied a systematic error to all float-based pCO_2 of ±1.8% (approximately 7.2 µatm; see Text S4). The resulting standard errors show that even if we account for a bias in the float-derived pCO_2 of this magnitude (which is twice the mean offset from the shipboard data), the float-based ASZ flux remains significantly higher than previous estimates, suggesting that this difference is robust.

4. Discussion

The substantial outgassing of CO_2 in the ASZ detected by the floats is consistent with the presence of upwelled deep water, rich in carbon and nutrients and depleted in oxygen [*Le Quéré et al.*, 2007; *Lovenduski et al.*, 2008; *Talley*, 2013]. Additional seawater properties observed by the floats support this hypothesis. Surface nitrate concentrations measured by the floats in the ASZ were significantly higher than nitrate concentrations estimated from a ship-based climatology [*Garcia et al.*, 2014] (Fig. S5). Compared to a ship-based climatology based on the same dataset as *Tak09* [*Takahashi et al.*, 2014], the floats measured considerably lower pH in the ASZ surface waters in winter, despite a negligible temperature difference [*Williams et al.*, 2018]. Analysis of float-based oxygen fluxes indicates a net oceanic uptake of oxygen in this region [*Bushinsky et al.*, 2017]. These findings, taken together with the substantial CO_2 flux to the atmosphere, provide evidence that the difference between the float-based ASZ flux and ship-based estimates is robust. Furthermore, this difference likely results from both interannual variability in the Southern Ocean CO_2 sink and an underestimation of wintertime outgassing due to biases in the distribution of shipboard observations.

Considerable changes in the Southern Ocean CO_2 flux have been observed previously on timescales of years to decades [*Le Quéré et al.*, 2007; *Landschützer et al.*, 2015], and such variability presumably plays a role in explaining the differences between the float results and prior estimates. Analysis of wind speeds and sea surface temperatures in the Southern Ocean shows that the winds were indeed stronger and temperatures colder in the both the PFZ and the ASZ during the float time period, compared to the climatological

average (Fig. S6). Both of these findings are consistent with an increase in wind-driven upwelling in this region, which would be expected to bring more carbon-rich deep water to the surface ocean and result in larger outgassing of CO_2 [*Lovenduski et al.*, 2008; *Le Quéré and Raupach*, 2009]. To estimate the impact of this variability, Fig. 3 gives the full range of the annual net regional fluxes in the *GCB17* estimate. Although variability of this magnitude can explain part of the difference found here, the ASZ float-based fluxes remain significantly higher than the upper end of the range in that ship-based estimate. Therefore interannual variability by itself appears inadequate to account for the entire 0.36 PgC y^{-1} difference between the float estimate and the ship-based flux in the ASZ.

The other likely cause of the persistent difference in the ASZ is that the ship-based estimates of CO_2 flux do not adequately capture the outgassing in this region due to a lack of wintertime data. Except for the Drake Passage region [*Munro et al.*, 2015], over the past decade there has been, on average, less than one cruise per year that measured pCO_2^{ocn} south of 50°S [*Bakker et al.*, 2016] in the austral winter, which is inadequate to properly resolve the seasonal cycle [*Fay et al.*, 2018]. Surface drifters measuring pCO_2 have previously been deployed in the Southern Ocean [*Boutin et al.*, 2008; *Barbero et al.*, 2011], but only a small fraction of that data was located in the ASZ. The substantial annual net flux found in the ASZ is produced almost entirely by strong outgassing in the late autumn to early spring (Figs. 2 and 3). The ship-based estimates, however, fail to capture this phenomenon, exhibiting only minimal wintertime outgassing. As a result, the annual net fluxes in the ASZ from those estimates agree, within the range of interannual variability, with the float-based fluxes averaged over summer only.

The strong outgassing in the upwelling region estimated from the float observations leads to a net annual CO_2 uptake of -0.08 PgC y^{-1} for the entire Southern Ocean south of 35°S (Table S2). The total uncertainty on this estimate, which stems from both spatio-temporal variability in the regional estimates and uncertainties associated with computation of the float-based fluxes, is dominated by potential systematic uncertainties in the float-derived pCO_2^{ocn}. Assuming the float-based pCO_2^{ocn} data are unbiased gave a lower-bound uncertainty estimate of ±0.04 PgC y^{-1}. An uncertainty estimate of ±0.55 PgC y^{-1} was calculated by stipulating, based on a thorough top-down uncertainty analysis [*Williams et al.*, 2017], that the mean error in the float-derived pCO_2^{ocn}, due to systematic uncertainties in the pH data, was normally-distributed with a standard deviation of 1.8% (approximately 7.2 µatm). However, the agreement of both the pH data and the float-derived pCO_2^{ocn} data with ship-based measurements [*Johnson et al.*, 2016, 2017; *Williams et al.*, 2017] suggests that systematic biases have been minimized by our approach and are likely less than 1.8%. Thus a standard error of ±0.55 PgC y^{-1} represents a reasonable upper-bound uncertainty on the total Southern Ocean CO_2 flux.

Even accounting for a possible systematic error in the float-derived pCO_2^{ocn}, the float-based Southern Ocean CO_2 flux estimate is considerably different from ship-based estimates that give a mean uptake of -0.8 (*Tak09*) or -0.9 (*GCB17*) PgC y^{-1} when sampled at the same locations at the floats. This finding has important implications regarding the distribution of CO_2 uptake in the climate system. If estimates of the total global oceanic uptake of CO_2 [e.g., *Gruber et al.*, 2009] are accurate, another oceanic region must be responsible for a stronger sink of CO_2 to compensate for the large source in the ASZ

found here. Inversions of existing atmospheric and interior ocean carbon observations often cannot statistically differentiate between carbon uptake in the Southern Ocean and uptake in the region between 18°S and 44°S [*Jacobson et al.*, 2007], suggesting a role for the Southern Hemisphere subtropical oceans. Alternatively, a reduction in the Southern Ocean CO_2 sink could be balanced by a change in terrestrial carbon fluxes.

Strong outgassing of CO_2 in the high-latitude Southern Ocean also has implications for global climate models. The majority predict oceanic fluxes in basic agreement with the standard estimate of a large Southern Ocean CO_2 sink, which is usually taken as a ground truth when evaluating models. One set of model experiments [*Rodgers et al.*, 2014], however, showed that adjusting upper ocean wind stirring in order to better reproduce observed summertime mixed layer depths led to substantial increases south of 45°S in CO_2 flux (0.9 PgC y^{-1} more outgassing) and surface NO_3 (up to 7 µmol kg^{-1} higher), indicating that inadequacies in the representation of mixing may be causing models to underestimate Southern Ocean CO_2 outgassing.

The float-based observations presented in this study suggest that in the upwelling region of the Southern Ocean, existing ship-based estimates likely underestimate the amplitude of the seasonal cycle of pCO_2^{ocn}, which leads to a substantial difference in total CO_2 uptake (Figs. 2 and 3). Over the next few years, as more and more biogeochemical floats are deployed in the Southern Ocean and globally [*Riser et al.*, 2016], new insights and knowledge will be gained by combining the relatively rare, but highly accurate, shipboard observations [*Bakker et al.*, 2016] with the complete annual cycles observed by floats. The significant outgassing of CO_2 in the high-latitude Southern Ocean found here, discov-

ered only with the extraordinary year-round data provided by these floats, presents an important challenge to our understanding of Southern Ocean's role in the global carbon cycle.

Acknowledgments. This work was sponsored by NSF's Southern Ocean Carbon and Climate Observations and Modeling (SOCCOM) Project under the NSF Award PLR-1425989 to J.L.S., supplemented by NASA (NNX14AP49G). Logistical support for SOCCOM in the Southern Ocean was provided by the U.S. National Science Foundation through the U.S. Antarctic Program and the U.S. GO-SHIP program, Australia's Commonwealth Scientific and Industrial Research Organisation (CSIRO), and Germany's Alfred Wegener Institute (AWI). Additionally, we acknowledge support from U.S. Argo through NOAA grant NA17RJ1232 to the University of Washington. A.R.G. was supported in part by a Climate and Global Change Postdoctoral Fellowship from the National Oceanic and Atmospheric Administration (NOAA). K.S.J acknowledges support from the David and Lucile Packard Foundation through the Monterey Bay Aquarium Research Institute. S.M.B. was supported in part by the Carbon Mitigation Initiative (CMI) project at Princeton University, sponsored by BP. Input from R. Feely, L. Juranek, B. Carter, A. Dickson and the SOCCOM carbon working group is gratefully acknowledged. We thank P. Landschützer for generously providing the Global Carbon Budget 2017 flux estimate.

All float data used in this study are archived at http://doi.org/10.6075/J0PG1PX7. Shipboard data used in calibration and adjustment are available at CCHDO (https://cchdo.ucsd.edu/) and CDIAC (http://cdiac.ornl.gov/oceans/SOCCOM/SOCCOM.html). ERA-Interim Reanalysis output was obtained from ECMWF (http://apps.ecmwf.int/datasets/)

and ASCAT daily gridded mean wind fields were downloaded from CERSAT (http://cersat.ifremer.fr/data/products/catalogue). Cape Grim Observatory data is available from CSIRO (http://www.csiro.au/greenhouse-gases). Sea ice data was retrieved from the National Snow and Ice Data Center (http://nsidc.org/data; Data Sets NSIDC-0051 and NSIDC-0081). Surface pCO_2 data were obtained from the Surface Ocean CO_2 Atlas (SOCAT; https://www.socat.info/), an international effort endorsed by the International Ocean Carbon Coordination Project (IOCCP), the Surface Ocean Lower Atmosphere Study (SOLAS) and the Integrated Marine Biogeochemistry and Ecosystem Research program (IMBER), to deliver a uniformly quality-controlled surface ocean CO_2 database. The many researchers and funding agencies responsible for the collection of data and quality control are thanked for their contributions to SOCAT. The gridded flux estimate from *Takahashi et al.* [2009] is available at http://www.ldeo.columbia.edu/res/pi/CO2/carbondioxide/pages/air_sea_flux_2000.html. The Global Carbon Budget 2017 air-sea flux estimate is available by contacting P. Landschützer. World Ocean Atlas 2013 gridded nitrate estimates were obtained from https://www.nodc.noaa.gov/OC5/woa13/woa13data.html, and the Roemmich-Gilson Argo Climatology is available from http://sio-argo.ucsd.edu/RG_Climatology.html.

References

Bakker, D. C. E., B. Pfeil, C. S. Landa, N. Metzl, K. M. OBrien, A. Olsen, K. Smith, C. Cosca, S. Harasawa, S. D. Jones, S. Nakaoka, Y. Nojiri, U. Schuster, T. Steinhoff, C. Sweeney, T. Takahashi, B. Tilbrook, C. Wada, R. Wanninkhof, S. R. Alin, C. F. Balestrini, L. Barbero, N. R. Bates, A. A. Bianchi, F. Bonou, J. Boutin, Y. Bozec, E. F.

Burger, W.-J. Cai, R. D. Castle, L. Chen, M. Chierici, K. Currie, W. Evans, C. Featherstone, R. A. Feely, A. Fransson, C. Goyet, N. Greenwood, L. Gregor, S. Hankin, N. J. Hardman-Mountford, J. Harlay, J. Hauck, M. Hoppema, M. P. Humphreys, C. W. Hunt, B. Huss, J. S. P. Ibnhez, T. Johannessen, R. Keeling, V. Kitidis, A. Krtzinger, A. Kozyr, E. Krasakopoulou, A. Kuwata, P. Landschtzer, S. K. Lauvset, N. Lefvre, C. Lo Monaco, A. Manke, J. T. Mathis, L. Merlivat, F. J. Millero, P. M. S. Monteiro, D. R. Munro, A. Murata, T. Newberger, A. M. Omar, T. Ono, K. Paterson, D. Pearce, D. Pierrot, L. L. Robbins, S. Saito, J. Salisbury, R. Schlitzer, B. Schneider, R. Schweitzer, R. Sieger, I. Skjelvan, K. F. Sullivan, S. C. Sutherland, A. J. Sutton, K. Tadokoro, M. Telszewski, M. Tuma, S. M. A. C. Van Heuven, D. Vandemark, B. Ward, A. J. Watson, and S. Xu (2016), A multi-decade record of high quality fCO_2 data in version 3 of the Surface Ocean CO_2 Atlas (SOCAT), *Earth Syst. Sci. Data*, *8*, 383–413, doi:10.5194/essd-8-383-2016.

Barbero, L., J. Boutin, L. Merlivat, N. Martin, T. Takahashi, S. C. Sutherland, and R. Wanninkhof (2011), Importance of water mass formation regions for the air-sea CO_2 flux estimate in the Southern Ocean, *Global Biogeochem. Cycles*, *25*(1), GB1005, doi:10.1029/2010GB003818.

Bentamya, A., and D. C. Fillona (2012), Gridded surface wind fields from Metop/ASCAT measurements, *Int. J. Remote Sens.*, *33*(6), 1729–1754, doi:10.1080/01431161.2011.600348.

Boebel, O. (2015), The Expedition PS89 of the Research Vessel POLARSTERN to the Weddell Sea in 2014/2015, *Tech. rep.*, Alfred Wegener Institute Report 689, http://doi.org/10.2312/BzPM_0689_2015.

Boutin, J., L. Merlivat, C. Hénocq, N. Martin, and J. B. Sallée (2008), Air-sea CO_2 flux variability in frontal regions of the Southern Ocean from CARbon Interface OCean Atmosphere drifters, *Limnol. Oceanogr.*, *53*, 2062–2079, doi:10.4319/lo.2008.53.5_part_2.2062.

Bushinsky, S. M., A. R. Gray, K. S. Johnson, and J. L. Sarmiento (2017), Oxygen in the Southern Ocean from Argo floats: Determination of processes driving air-sea fluxes, *J. Geophys. Res. Oceans*, *122*(11), 8661–8682, doi:10.1002/2017JC012923.

Carter, B. R., R. A. Feely, N. L. Williams, A. G. Dickson, M. B. Fong, and Y. Takeshita (2018), Updated methods for global locally interpolated estimation of alkalinity, pH, and nitrate, *Limnol. Oceanogr.-Meth.*, *16*(2), 119–131, doi:10.1002/lom3.10232.

Cavalieri, D. J., C. L. Parkinson, P. Gloersen, and H. J. Zwally (1996), Sea Ice Concentrations from Nimbus-7 SMMR and DMSP SSM/I-SSMIS Passive Microwave Data, Version 1., *Tech. rep.*, NASA National Snow and Ice Data Center Distributed Active Archive Center doi:10.5067/8GQ8LZQVL0VL, accessed 01/09/2016.

Chaudhuri, A. H., R. M. Ponte, G. Forget, and P. Heimbach (2013), A comparison of atmospheric reanalysis surface products over the ocean and implications for uncertainties in air-sea boundary forcing, *J. Climate*, *26*(1), 153–170, doi:10.1175/JCLI-D-12-00090.1.

Cofin, M. F. (2016), RV Investigator Voyage Summary, Voyage IN2016_v01, *Tech. rep.*, Commonwealth Scientific and Industrial Research Organisation, https://soccom.princeton.edu/sites/default/files/media/pdf/IN2016_V01_Voyage_Summary_20160616.pdf.

de Boyer Montégut, C., G. Madec, A. S. Fischer, A. Lazar, and D. Iudicone (2004), Mixed layer depth over the global ocean: An examination of profile data and a profile-based climatology, *J. Geophys. Res. Oceans*, *109*(12), doi:10.1029/2004JC002378.

Dee, D. P., S. M. Uppala, A. J. Simmons, P. Berrisford, P. Poli, S. Kobayashi, U. Andrae, M. A. Balmaseda, G. Balsamo, P. Bauer, P. Bechtold, A. C. M. Beljaars, L. van de Berg, J. Bidlot, N. Bormann, C. Delsol, R. Dragani, M. Fuentes, A. J. Geer, L. Haimberger, S. B. Healy, H. Hersbach, E. V. Hólm, L. Isaksen, P. Kållberg, M. Köhler, M. Matricardi, A. P. McNally, B. M. Monge-Sanz, J.-J. Morcrette, B.-K. Park, C. Peubey, P. de Rosnay, C. Tavolato, J.-N. Thépaut, and F. Vitart (2011), The ERA-Interim reanalysis: Configuration and performance of the data assimilation system, *Q. J. Roy. Meteor. Soc.*, *137*(656), 553–597, doi:10.1002/qj.828.

Dickson, A. G. (1990), Thermodynamics of the dissociation of boric acid in synthetic seawater from 273.15 to 318.15 K, *Deep-Sea Res.*, *37*(5), 755–766, doi:10.1016/0198-0149(90)90004-F.

Fay, A. R., N. S. Lovenduski, G. A. McKinley, D. R. Munro, C. Sweeney, A. R. Gray, P. Landschützer, B. B. Stephens, T. Takahashi, and N. Williams (2018), Utilizing the Drake Passage Time-series to understand variability and change in subpolar Southern Ocean pCO_2, *Biogeosciences*, *15*(12), 3841–3855, doi:10.5194/bg-15-3841-2018.

Firing, Y. (2016), RRS James Clark Ross Cruise JR15003, *Tech. rep.*, National Oceanography Centre, Cruise Report No. 38, https://cchdo.ucsd.edu/data/12275/NOC_CR_38.pdf.

Frölicher, T. L., J. L. Sarmiento, D. J. Paynter, J. P. Dunne, J. P. Krasting, and M. Winton (2015), Dominance of the Southern Ocean in anthropogenic carbon and heat uptake in CMIP5 models, *J. Climate*, *28*(2), 862–886, doi:10.1175/JCLI-D-14-00117.1.

Garcia, H. E., R. A. Locarnini, T. P. Boyer, J. I. Antonov, O. Baranova, M. Zweng, J. Reagan, and D. Johnson (2014), World Ocean Atlas 2013, Volume 4: Dissolved Inorganic Nutrients (phosphate, nitrate, silicate), *Tech. rep.*, NOAA Atlas NESDIS 76.

Gruber, N., M. Gloor, S. E. M. Fletcher, S. C. Doney, S. Dutkiewicz, M. J. Follows, M. Gerber, A. R. Jacobson, F. Joos, K. Lindsay, D. Menemenlis, A. Mouchet, S. A. Mueller, J. L. Sarmiento, and T. Takahashi (2009), Oceanic sources, sinks, and transport of atmospheric CO_2, *Global Biogeochem. Cycles*, *23*, GB1005, doi:{10.1029/2008GB003349}.

Jacobson, A. R., S. E. M. Fletcher, N. Gruber, J. L. Sarmiento, and M. Gloor (2007), A joint atmosphere-ocean inversion for surface fluxes of carbon dioxide: 2. Regional results, *Global Biogeochem. Cycles*, *21*(1), 1–15, doi:10.1029/2006GB002703.

Johnson, K. S., L. J. Coletti, H. W. Jannasch, C. M. Sakamoto, D. D. Swift, and S. C. Riser (2013), Long-term nitrate measurements in the ocean using the in situ ultraviolet spectrophotometer: Sensor integration into the APEX profiling float, *J. Atmos. Ocean. Tech.*, *30*(8), 1854–1866, doi:10.1175/JTECH-D-12-00221.1.

Johnson, K. S., J. N. Plant, S. C. Riser, and D. Gilbert (2015), Air oxygen calibration of oxygen optodes on a profiling float array, *J. Atmos. Ocean. Tech.*, *32*(11), 2160–2172, doi:10.1175/JTECH-D-15-0101.1.

Johnson, K. S., H. W. Jannasch, L. J. Coletti, V. A. Elrod, T. R. Martz, Y. Takeshita, R. J. Carlson, and J. G. Connery (2016), Deep-Sea DuraFET: A pressure tolerant pH sensor designed for global sensor networks, *Anal. Chem.*, *88*, 3429–3256, doi:10.1021/acs.analchem.5b04653.

Johnson, K. S., J. N. Plant, L. J. Coletti, H. W. Jannasch, C. M. Sakamoto, S. C. Riser, D. D. Swift, N. L. Williams, E. Boss, N. Haëntjens, L. D. Talley, and J. L. Sarmiento (2017), Biogeochemical sensor performance in the SOCCOM profiling float array, *J. Geophys. Res.: Oceans*, *122*, doi:10.1002/2017JC012838.

Johnson, K. S., S. C. Riser, E. S. Boss, L. D. Talley, J. L. Sarmiento, D. D. Swift, J. N. Plant, T. L. Maurer, R. M. Key, N. L. Williams, R. H. Wanninkhof, A. G. Dickson, R. A. Feely, and J. L. Russell (2018), SOCCOM float data - Snapshot 2018-03-06, In Southern Ocean Carbon and Climate Observations and Modeling (SOCCOM) Float Data Archive, doi:10.6075/J0PG1PX7.

Kalnay, E., M. Kanamitsu, R. Kistler, W. Collins, D. Deaven, L. Gandin, M. Iredell, S. Saha, G. White, J. Woollen, Y. Zhu, A. Leetmaa, R. Reynolds, M. Chelliah, W. Ebisuzaki, W. Higgins, J. Janowiak, K. C. Mo, C. Ropelewski, J. Wang, R. Jenne, and D. Joseph (1996), The NCEP/NCAR 40-Year reanalysis project, *B. Am. Meteorol. Soc.*, *77*(3), 437–471, doi:10.1175/1520-0477(1996)077⟨0437:TNYRP⟩2.0.CO;2.

Landschützer, P., N. Gruber, and D. Bakker (2015), A 30 years observation-based global monthly gridded sea surface pCO_2 product from 1982 through 2011, *Tech. rep.*, Carbon Dioxide Information Analysis Center, Oak Ridge National Laboratory, US Department of Energy, Oak Ridge, Tennessee

doi:10.3334/CDIAC/OTG.SPCO2_1982_2011_ETH_SOM-FFN.

Landschützer, P., N. Gruber, D. C. E. Bakker, and U. Schuster (2014), Recent variability of the global ocean carbon sink, *Global Biogeochem. Cycles*, *28*(9), 927–949, doi:10.1002/2014GB004853.

Landschützer, P., N. Gruber, A. Haumann, C. Rodenbeck, D. C. E. Bakker, S. van Heuven, M. Hoppema, N. Metzl, C. Sweeney, T. Takahashi, B. Tilbrook, and R. Wanninkhof (2015), The reinvigoration of the Southern Ocean carbon sink, *Science*, *349*(6253), 1221–1224, doi:10.1126/science.aab2620.

Le Quéré, C., and M. Raupach (2009), Trends in the sources and sinks of carbon dioxide, *Nat. Geosci.*, *2*, 1–6, doi:10.1038/NGEO689.

Le Quéré, C., C. Rödenbeck, E. T. Buitenhuis, T. J. Conway, R. Langenfelds, A. Gomez, C. Labuschagne, M. Ramonet, T. Nakazawa, N. Metzl, N. Gillett, and M. Heimann (2007), Saturation of the southern ocean CO_2 sink due to recent climate change., *Science*, *316*(5832), 1735–1738, doi:10.1126/science.1136188.

Le Quéré, C., R. M. Andrew, P. Friedlingstein, S. Sitch, J. Pongratz, A. C. Manning, J. Ivar Korsbakken, G. P. Peters, J. G. Canadell, R. B. Jackson, T. A. Boden, P. P. Tans, O. D. Andrews, V. K. Arora, D. C. Bakker, L. Barbero, M. Becker, R. A. Betts, L. Bopp, F. Chevallier, L. P. Chini, P. Ciais, C. E. Cosca, J. Cross, K. Currie, T. Gasser, I. Harris, J. Hauck, V. Haverd, R. A. Houghton, C. W. Hunt, G. Hurtt, T. Ilyina, A. K. Jain, E. Kato, M. Kautz, R. F. Keeling, K. Klein Goldewijk, A. Körtzinger, P. Landschützer, N. Lefèvre, A. Lenton, S. Lienert, I. Lima, D. Lombardozzi, N. Metzl, F. Millero, P. M. Monteiro, D. R. Munro, J. E. Nabel, S. I. Nakaoka, Y. Nojiri, X. Antonio Padin,

A. Peregon, B. Pfeil, D. Pierrot, B. Poulter, G. Rehder, J. Reimer, C. Rödenbeck, J. Schwinger, R. Séférian, I. Skjelvan, B. D. Stocker, H. Tian, B. Tilbrook, F. N. Tubiello, I. T. Laan-Luijkx, G. R. Werf, S. Van Heuven, N. Viovy, N. Vuichard, A. P. Walker, A. J. Watson, A. J. Wiltshire, S. Zaehle, and D. Zhu (2018), Global Carbon Budget 2017, *Earth Syst. Sci. Data*, *10*(1), 405–448, doi:10.5194/essd-10-405-2018.

Lee, K., T.-W. Kim, R. H. Byrne, F. J. Millero, R. A. Feely, and Y.-M. Liu (2010), The universal ratio of boron to chlorinity for the North Pacific and North Atlantic oceans, *Geochim. Cosmochim. Ac.*, *74*(6), 1801–1811, doi:10.1016/j.gca.2009.12.027.

Lenton, A., B. Tilbrook, R. M. Law, D. Bakker, S. C. Doney, N. Gruber, M. Ishii, M. Hoppema, N. S. Lovenduski, R. J. Matear, B. I. McNeil, N. Metzl, S. E. M. Fletcher, P. M. S. Monteiro, C. Roedenbeck, C. Sweeney, and T. Takahashi (2013), Sea-air CO_2 fluxes in the Southern Ocean for the period 1990-2009, *Biogeosciences*, *10*(6), 4037–4054, doi:10.5194/bg-10-4037-2013.

Lovenduski, N. S., N. Gruber, and S. C. Doney (2008), Toward a mechanistic understanding of the decadal trends in the Southern Ocean carbon sink, *Global Biogeochem. Cycles*, *22*(3), GB3016, doi:10.1029/2007GB003139.

Lueker, T. J., A. G. Dickson, and C. D. Keeling (2000), Ocean pCO_2 calculated from dissolved inorganic carbon, alkalinity, and equations for K_1 and K_2: Validation based on laboratory measurements of CO_2 in gas and seawater at equilibrium, *Mar. Chem.*, *70*(1), 105–119, doi:10.1016/S0304-4203(00)00022-0.

Lumpkin, R., and K. Speer (2007), Global ocean meridional overturning, *J. Phys. Oceanogr.*, *37*(10), 2550–2562, doi:10.1175/JPO3130.1.

MacDonald, A. (2016), Cruise Report of the 2016 I08S US GO-SHIP Reoccupation, *Tech. rep.*, U.S. GO-SHIP, https://cchdo.ucsd.edu/data/12419/33RR20160208_do.pdf.

Marshall, J., and K. Speer (2012), Closure of the meridional overturning circulation through Southern Ocean upwelling, *Nat. Geoscience*, *5*(3), 171–180, doi:10.1038/ngeo1391.

Meijers, A. J. S. (2014), The Southern Ocean in the Coupled Model Intercomparison Project phase5., *Philos. Trans. R. Soc., A*, *372*(2019), 20130,296, doi:10.1098/rsta.2013.0296.

Munro, D. R., N. S. Lovenduski, T. Takahashi, B. B. Stephens, T. Newberger, and C. Sweeney (2015), Recent evidence for a strengthening CO_2 sink in the Southern Ocean from carbonate system measurements in the Drake Passage (2002-2015), *Geophys. Res. Lett.*, *42*(18), 7623–7630, doi:10.1002/2015GL065194.

Nevison, C. D., M. Manizza, R. F. Keeling, B. B. Stephens, J. D. Bent, J. Dunne, T. Ilyina, M. Long, L. Resplandy, J. Tjiputra, and S. Yukimoto (2016), Evaluating CMIP5 ocean biogeochemistry and Southern Ocean carbon uptake using atmospheric potential oxygen: Present-day performance and future projection, *Geophys. Res. Lett.*, *43*(5), 2077–2085, doi:10.1002/2015GL067584.

Orsi, A. H., T. Whitworth, and W. D. Nowlin (1995), On the meridional extent and fronts of the Antarctic Circumpolar Current, *Deep-Sea Res. Pt. I*, *42*(5), 641–673, doi:10.1016/0967-0637(95)00021-W.

Perez, F. F., and F. Fraga (1987), Association constant of fluoride and hydrogen ions in seawater, *Mar. Chem.*, *21*(2), 161–168, doi:10.1016/0304-4203(87)90036-3.

Riser, S. C., H. J. Freeland, D. Roemmich, S. Wijffels, A. Troisi, M. Belbéoch, D. Gilbert, J. Xu, S. Pouliquen, A. Thresher, P.-Y. Le Traon, G. Maze, B. Klein, M. Ravichandran, F. Grant, P.-M. Poulain, T. Suga, B. Lim, A. Sterl, P. Sutton, K.-A. Mork, P. J. Vélez-Belchí, I. Ansorge, B. King, J. Turton, M. Baringer, and S. R. Jayne (2016), Fifteen years of ocean observations with the global Argo array, *Nat. Clim. Change*, *6*(2), 145–153, doi:10.1038/nclimate2872.

Risien, C. M., and D. B. Chelton (2008), A global climatology of surface wind and wind stress fields from eight years of QuikSCAT scatterometer data, *J. Phys. Oceanogr.*, *38*(11), 2379–2413, doi:10.1175/2008JPO3881.1.

Rodgers, K. B., O. Aumont, S. E. Mikaloff Fletcher, Y. Plancherel, L. Bopp, C. De Boyer Montégut, D. Iudicone, R. F. Keeling, G. Madec, and R. Wanninkhof (2014), Strong sensitivity of Southern Ocean carbon uptake and nutrient cycling to wind stirring, *Biogeosciences*, *11*(15), 4077–4098, doi:10.5194/bg-11-4077-2014.

Roemmich, D., and J. Gilson (2009), The 2004-2008 mean and annual cycle of temperature, salinity, and steric height in the global ocean from the Argo Program, *Prog. Oceanogr.*, *82*, 81–100, doi:10.1016/j.pocean.2009.03.004.

Salstein, D. A., R. M. Ponte, and K. Cady-Pereira (2008), Uncertainties in atmospheric surface pressure fields from global analyses, *J. Geophys. Res.*, *113*, D14,107, doi:10.1029/2007JD009531.

Sigman, D. M., M. P. Hain, and G. H. Haug (2010), The polar ocean and glacial cycles in atmospheric CO_2 concentration, *Nature*, *466*(7302), 47–55, doi:10.1038/nature09149.

Sloyan, B., and S. Wijffels (2016), RV Investigator Voyage Summary, Voyage IN2016_v03, *Tech. rep.*, Commonwealth Scientific and Industrial Research Organisation, https://cchdo.ucsd.edu/data/12704/096U20160426_do.pdf.

Takahashi, T., S. C. Sutherland, C. Sweeney, A. Poisson, N. Metzl, B. Tilbrook, N. Bates, R. Wanninkhof, R. A. Feely, C. Sabine, J. Olafsson, and Y. Nojiri (2002), Global sea-air CO_2 flux based on climatological surface ocean pCO_2 and seasonal biological and temperature effects, *Deep-Sea Res. Pt. II*, *49*(9-10), 1601–1622, doi: 10.1016/S0967-0645(02)00003-6.

Takahashi, T., S. Sutherland, D. Chipman, J. Goddard, C. Ho, T. Newberger, C. Sweeney, and D. Munro (2014), Climatological distributions of pH, pCO2, total CO2, alkalinity, and CaCO3 saturation in the global surface ocean, and temporal changes at selected locations, *Mar. Chem.*, *164*, 95–125, doi:10.1016/J.MARCHEM.2014.06.004.

Takahashi, T., S. C. Sutherland, R. Wanninkhof, C. Sweeney, R. A. Feely, D. W. Chipman, B. Hales, G. Friederich, F. Chavez, C. Sabine, A. Watson, D. C. E. Bakker, U. Schuster, N. Metzl, H. Yoshikawa-Inoue, M. Ishii, T. Midorikawa, Y. Nojiri, A. Koertzinger, T. Steinhoff, M. Hoppema, J. Olafsson, T. S. Arnarson, B. Tilbrook, T. Johannessen, A. Olsen, R. Bellerby, C. S. Wong, B. Delille, N. R. Bates, and H. J. W. de Baar (2009), Climatological mean and decadal change in surface ocean pCO_2 and net sea-air CO_2 flux over the global oceans, *Deep-Sea Res. Pt. II*, *56*(8-10), 554–577, doi: 10.1016/j.dsr2.2008.12.009.

Talley, L. D. (2013), Closure of the global overturning circulation through the Indian, Pacific, and Southern Oceans: Schematics and transports, *Oceanography*, *26*(1), 80–97,

doi:10.5670/oceanog.2013.07.

Talley, L. D., K. S. Johnson, S. C. Riser, and T. C. Hennon (2014), SOCCOM biogeochemical profiling float deployments from GO-SHIP P16S (RVIB Nathaniel B. Palmer NBP1403), *Tech. rep.*, SOCCOM Tech. Rep. 2014-1, http://soccom.princeton.edu/sites/default/files/files/SOCCOM_2014-1_P16S_floats.pdf.

Tengberg, A., J. Hovdenes, H. J. Andersson, O. Brocandel, R. Diaz, D. Hebert, T. Arnerich, C. Huber, A. Körtzinger, A. Khripounoff, F. Rey, C. Rönning, J. Schimanski, S. Sommer, and A. Stangelmayer (2006), Evaluation of a lifetime-based optode to measure oxygen in aquatic systems, *Limnol. Oceanogr.-Meth.*, *4*, 7–17, doi:10.4319/lom.2006.4.7.

Trull, T. (2015), RV Investigator Voyage Summary, Voyage IN2015_v01, *Tech. rep.*, Commonwealth Scientific and Industrial Research Organisation, http://soccom.princeton.edu/sites/default/files/files/IN2015_v01_Voyage_Summary_Chief_Scientist.pdf.

Trull, T. (2016), RV Investigator Voyage Summary, Voyage IN2016_v02, *Tech. rep.*, Commonwealth Scientific and Industrial Research Organisation, https://soccom.princeton.edu/sites/default/files/files/IN2016_V02_VoyagePlan_SubmissiontoMNF_11Dec2015.pdf.

Wanninkhof, R. (2014), Relationship between wind speed and gas exchange over the ocean revisited, *Limnol. Oceanogr.-Meth.*, *12*, 351–361, doi:10.4319/lom.2014.12.351.

Wanninkhof, R., K. Johnson, N. Williams, J. Sarmiento, S. Riser, E. Briggs, S. Bushinsky, B. Carter, A. Dickson, R. Feely, A. Gray, L. Juranek, R. Key, L. Talley, J. Russels, and A. Verdy (2016), An evaluation of pH and NO_3 sensor data from SOCCOM floats and their utilization to develop ocean inorganic carbon products, *Tech. rep.*, SOCCOM Carbon System Working Group, http://soccom.princeton.edu/sites/default/files/files/CWG_white_paper_March_13_2016.pdf.

Weiss, R. (1974), Carbon dioxide in water and seawater: The solubility of a non-ideal gas, *Mar. Chem.*, *2*(3), 203–215, doi:10.1016/0304-4203(74)90015-2.

Weller, R. (2015), Global Southern Ocean 1 Deployment, *Tech. rep.*, Ocean Observatories Initiative, No. 3201-00102, https://alfresco.oceanobservatories.org/alfresco/d/d/workspace/SpacesStore/c5d98550-f51a-47d2-be05-d45165c73835/3201-00102_Quick_Look_Report_Southern_Ocean_1_2015-05-26_Ver_1-00.pdf.

Williams, N. L., L. W. Juranek, K. S. Johnson, R. A. Feely, S. C. Riser, L. D. Talley, J. L. Russell, J. L. Sarmiento, and R. Wanninkhof (2016), Empirical algorithms to estimate water column pH in the Southern Ocean, *Geophys. Res. Lett.*, *43*(7), 3415–3422, doi:10.1002/2016GL068539.

Williams, N. L., L. W. Juranek, R. A. Feely, K. S. Johnson, J. L. Sarmiento, L. D. Talley, A. G. Dickson, A. R. Gray, R. Wanninkhof, J. L. Russell, and S. C. Riser (2017), Calculating surface ocean pCO_2 from biogeochemical Argo floats equipped with pH: An uncertainty analysis, *Global Biogeochem. Cycles*, *31*, 591–604, doi:10.1002/2016GB005541.

Williams, N. L., L. W. Juranek, R. A. Feely, J. L. Russell, K. S. Johnson, and B. Hales (2018), Assessment of the carbonate chemistry seasonal cycles in the southern ocean from persistent observational platforms, *J. Geophys. Res. Oceans*, *in press*, doi:10.1029/2017JC012917.

Wong, A. P. S., and S. C. Riser (2011), Profiling float observations of the upper ocean under sea ice off the Wilkes Land coast of Antarctica, *J. Phys. Oceanogr.*, *41*(6), 1102–1115, doi:10.1175/2011JPO4516.1.

Zeebe, R. E., and D. A. Wolf-Gladrow (2001), *CO_2 in Seawater: Equilibrium, Kinetics, Isotopes*, Elsevier Oceanography Series, 65, Elsevier.

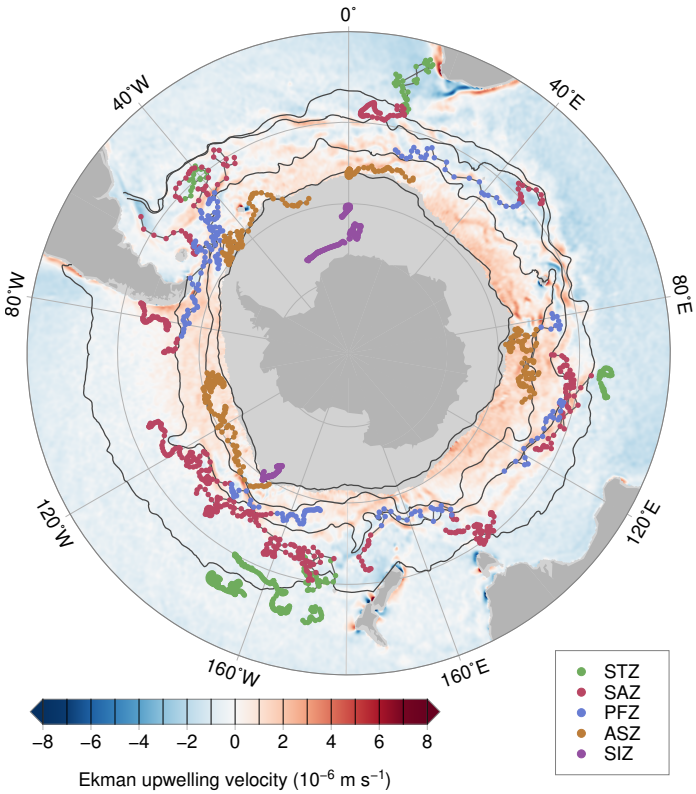

Figure 1. Profile locations from 35 autonomous biogeochemical floats deployed in the Southern Ocean [*Talley et al.*, 2014; *Boebel*, 2015; *Trull*, 2015; *Weller*, 2015; *Cofin*, 2016; *Firing*, 2016; *Trull*, 2016; *MacDonald*, 2016; *Sloyan and Wijffels*, 2016] from 1 May 2014 through 1 May 2017, colored according to zone. Dark gray contours show the boundaries of the five regions used in the analysis (see Text S3). Background colors show the annual mean wind-induced upwelling velocity, calculated from the Scatterometer Climatology of Ocean Winds [*Risien and Chelton*, 2008], with light gray indicating the region covered by both seasonal and permanent sea ice in that climatology.

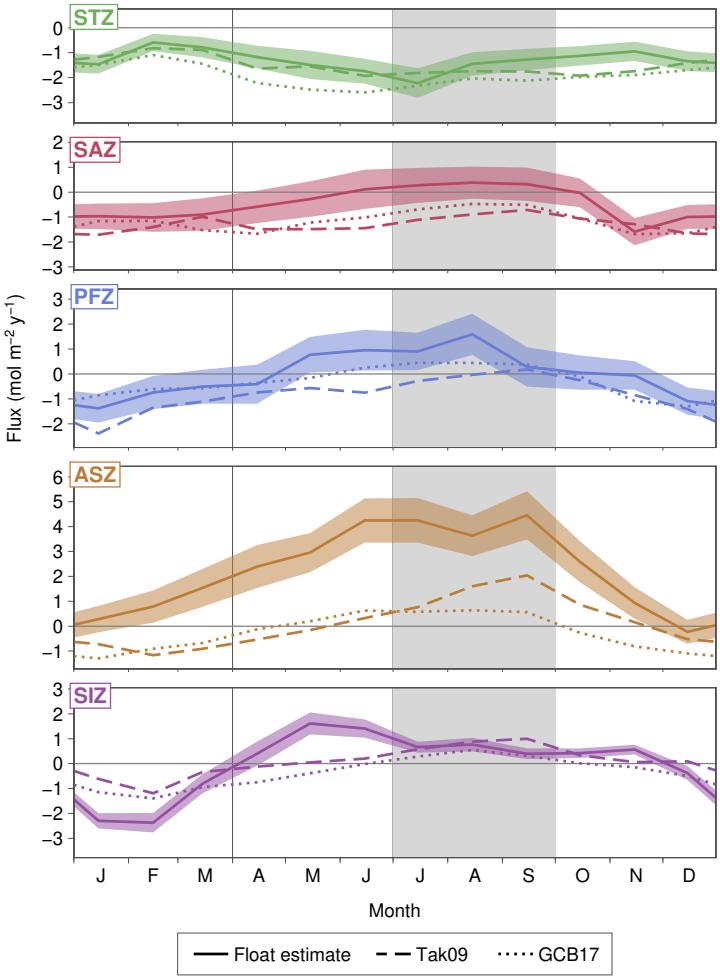

Figure 2. Monthly mean air-sea fluxes of CO_2 in each zone, computed from float observations, atmospheric CO_2 measurements, and wind speed estimates (solid lines). The shading represents ± 1 standard error, calculated using a Monte Carlo simulation of the associated uncertainties (see Text S4). The mean monthly fluxes from *Tak09* (dashed lines) and *GCB17* (dotted lines) were calculated by sampling those estimates at the locations of the floats and averaging the resulting monthly mean fluxes as for the float data. Positive (negative) denotes flux out of (into) the ocean. Light gray vertical bar highlights winter months (JAS).

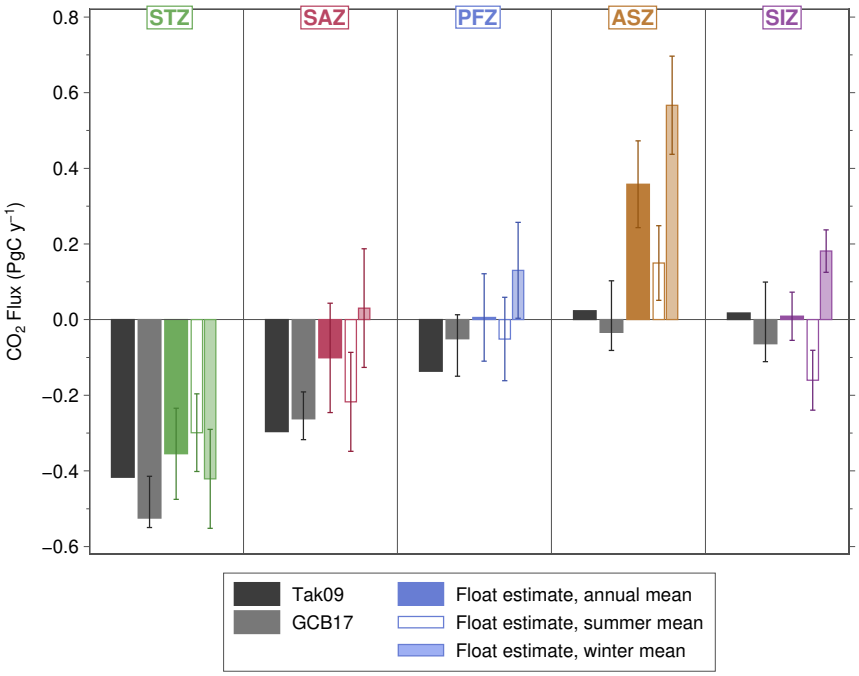

Figure 3. Annual net oceanic CO_2 flux (PgC y^{-1}) estimated from float data (solid colors) and from two ship-based estimates, *Tak09* (dark gray) and *GCB17* (light gray), calculated by sampling the gridded estimates at the same locations as the floats. Uncertainty on the float estimates represents ±1 standard error, with contributions due to both spatio-temporal variability in the CO_2 flux and uncertainties in the data assessed with a Monte Carlo simulation (see Text S4). Error bars on the *GCB17* data indicate the range of interannual variability across that 35-year estimate. The mean float-based estimates calculated for May-October (winter) and for November-April (summer) are shown by the narrow bars. Positive (negative) indicates net outgassing (uptake).

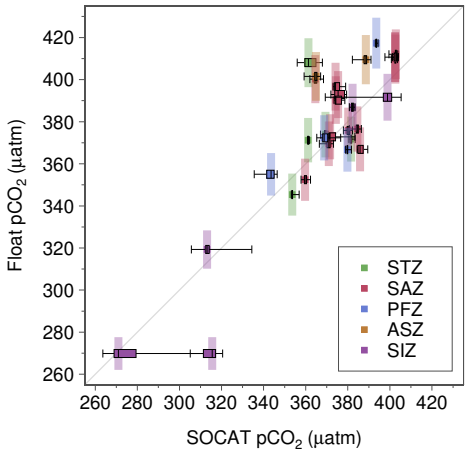

Figure 4. Comparison between measured pCO_2^{ocn} from SOCAT v5 [*Bakker et al.*, 2016] and calculated pCO_2^{ocn} from the floats used in this study (averaged in the upper 20 m). Box-and-whiskers give the median, interquartile range, and minimum and maximum of all underway ship-board data within 25 km and 1 day of the float profile. Lighter shading gives the uncertainty estimate (± 1 standard error) on the float pCO_2^{ocn}. Colors indicate the zone of the float measurement, and the gray line represents the one-to-one relationship.